hep-ph/0111064
CERN–TH/2001-291
UMN–TH–2029/01
TPI–MINN–01/47

Constraints from Accelerator Experiments on the Elastic Scattering of CMSSM Dark Matter

John Ellis[1], **Andrew Ferstl**[2] and **Keith A. Olive**[3]

[1] *TH Division, CERN, Geneva, Switzerland*

[2] *Department of Physics, Winona State University, Winona, MN 55987, USA*

[3] *Theoretical Physics Institute, University of Minnesota, Minneapolis, MN 55455, USA*

Abstract

We explore the allowed ranges of cross sections for the elastic scattering of neutralinos χ on nucleons in the constrained minimal supersymmetric extension of the Standard Model (CMSSM), in which scalar and gaugino masses are each assumed to be universal at some input grand unification scale. We extend previous calculations to larger $\tan\beta$ and investigate the limits imposed by the recent LEP lower limit on the mass of the Higgs boson and by $b \to s\gamma$, and those suggested by $g_\mu - 2$. The Higgs limit and $b \to s\gamma$ provide upper limits on the cross section, particularly at small and large $\tan\beta$, respectively, and the value of $g_\mu - 2$ suggests a lower limit on the cross section for $\mu > 0$. The spin-independent nucleon cross section is restricted to the range 6×10^{-8} pb$> \sigma_{SI} > 2 \times 10^{-10}$ pb for $\mu > 0$, and the spin-dependent nucleon cross section to the range 10^{-5} pb$> \sigma_{SD} > 2 \times 10^{-7}$ pb. Lower values are allowed if $\mu < 0$.

CERN–TH/2001-291
October 2001

One of the front-running candidates for cold dark matter is the lightest supersymmetric particle (LSP), which is often taken to be the lightest neutralino χ [1]. Several experiments looking for the scattering of cold dark matter particles on nuclear targets [2] have reached a sensitivity to a spin-independent elastic cross section σ_{SI} of the order of 10^{-5} pb for $m_\chi \sim 100$ GeV [3], and one experiment has reported a possible positive signal [4]. A new generation of more sensitive experiments is now being prepared and proposed, with sensitivities extending as low as 3×10^{-9} pb [5]. It is therefore important to update theoretical predictions for the elastic scattering cross section, including the spin-dependent component, σ_{SD}, as well as the spin-independent part, σ_{SI}.

The cross-section ranges allowed in the general minimal supersymmetric extension of the Standard Model (MSSM) are quite broad, being sensitive to the Higgs and squark masses, in particular [6, 7]. It is common to focus attention on the constrained MSSM (CMSSM), in which all the soft supersymmetry-breaking scalar masses m_0 are required to be equal at an input superysmmetric GUT scale, as are the gaugino masses $m_{1/2}$ and the trilinear soft supersymmetry-breaking parameters A. These assumptions yield well-defined relations between the various sparticle masses, and correspondingly more definite predictions for the elastic χ-nucleon scattering cross sections as functions of m_χ [8]. This paper is devoted to an updated discussion of σ_{SI} and σ_{SD} in the CMSSM as functions of m_0, $m_{1/2}$, and $\tan\beta$ for $A = 0$.

This is timely in view of two significant experimental developments since our previous analysis [7]. One has been the improvement in the experimental lower limit from LEP on the mass of the lightest MSSM Higgs boson h [9], which is now $m_h > 114.1$ GeV in the context of the CMSSM [1]. The second major experimental development has been the report of a possible 2.6 - σ discrepancy between the measured and Standard Model values of the anomalous magnetic moment of the muon, $a_\mu \equiv (g_\mu - 2)/2$: $a_\mu = (43 \pm 16) \times 10^{-10}$ [10], which we interpret as $11 \times 10^{-10} < a_\mu < 75 \times 10^{-10}$. The supersymmetric interpretation [11, 12] of this result is not yet established: it could be that strong-interaction uncertainties in the Standard Model prediction have been underestimated, or there might have been a statistical fluctuation in the data. Even if the discrepancy is confirmed, it might be evidence for some other type of physics beyond the Standard Model. Nevertheless, we are tempted to explore its possible consequences for dark matter scattering within the CMSSM context [13].

Theoretically, there have also been improvements recently in the calculations in the CMSSM of the supersymmetric relic density $\Omega_\chi h^2$ for large values of the ratio $\tan\beta$ of

[1] In the general MSSM, m_h could be as low as ~ 90 GeV, but this is only possible for variants in which the $Z - Z - h$ coupling is suppressed to an extent that does not occur within the CMSSM as studied here.

Higgs vacuum expectation values [14]. These define better the interesting region of CMSSM parameter space where the relic density may fall within the range $0.1 < \Omega_\chi h^2 < 0.3$ preferred by astrophysics and cosmology [15].

We find that the expected ranges of both the spin-independent cross sections σ_{SI} and the spin-dependent cross sections σ_{SD} in the CMSSM are quite restricted (see also [16]). The LEP Higgs limit [9] sets upper bounds on σ_{SI} and σ_{SD}, not only via the direct contribution of Higgs exchange to the scattering matrix element, but also because it provides a strong lower limit on m_χ at low $\tan\beta$, in particular [17].[2] At high $\tan\beta$, the observed rate of $b \to s\gamma$ also provides [18] an important lower limit on m_χ and hence an upper limit on $\sigma_{SI,SD}$ [19]. In view of these upper limits, we are unable to provide a CMSSM interpetation of the DAMA signal [4]. More excitingly for prospective experiments, the range $11 \times 10^{-10} < a_\mu < 75 \times 10^{-10}$ would imply important upper limits on sparticle masses, and hence a *lower limit*: $\sigma_{SI} > 2 \times 10^{-10}$ pb. Putting together all the constraints, we find for $\mu > 0$ a relatively narrow band 6×10^{-8} pb $> \sigma_{SI} > 2 \times 10^{-10}$ pb. The allowed range is typically broadest at large $\tan\beta$. Lower cross sections are possible if $\mu < 0$.

As has been discussed in detail elsewhere, the regions of $m_{1/2}, m_0$ plane where the relic density falls within the preferred range $0.1 < \Omega_\chi h^2 < 0.3$ can be divided into four generic parts, whose relative significances depend on $\tan\beta$. There is a 'bulk' region at moderate $m_{1/2}$ and m_0 [1], where supersymmetry is relatively easy to detect at colliders and as dark matter. Then, extending to larger $m_{1/2}$, there is a 'tail' of the parameter space where the LSP χ is almost degenerate with the next-to-lightest supersymmetric particle (NLSP), and efficient coannihilations [20] keep $\Omega_\chi h^2$ in the preferred range, even for larger values of m_χ [21]. At larger m_0, close to the boundary where electroweak symmetry breaking is no longer possible, there is the 'focus-point' region where the LSP has a more prominent Higgsino component and m_χ is small enough for $\Omega_\chi h^2$ to be acceptable [22]. Finally, extending to larger $m_{1/2}$ and m_0 at intermediate values of $m_{1/2}/m_0$, there may be a 'funnel' of CMSSM parameter space where rapid direct-channel annihilations via the poles of the heavier Higgs bosons A and H may keep $\Omega_\chi h^2$ in the preferred range [14, 23]. In this paper, we focus on the case $A = 0$ and use the `SSARD` code to calculate the relic density [24]. The precise values of $m_{1/2}$ and m_0 in the 'focus-point' and 'funnel' regions are quite sensitive to the precise values and treatments of the input CMSSM and other parameters [25, 26]. These regions are not emphasized in the following discussion, but are commented upon where appropriate.

The code we use to calculate the elastic dark matter scattering cross sections $\sigma_{SI,SD}$ was

[2] Apart from cancellations that occur in σ_{SD} when $\mu < 0$, the elastic cross sections are monotonically decreasing functions of m_χ in the CMSSM [8].

documented in [8, 7], together with the ranges of values of the hadronic matrix elements that we use. The cross sections for protons and neutrons are similar within the quoted uncertainties in these matrix elements. Codes are available [27] that include additional contributions to the scattering matrix elements, but a recent comparison [28] shows that the improvements are not essential in the CMSSM parameter space that we explore here. Fig. 1 displays contours of the spin-independent cross section for the elastic scattering of the LSP χ on protons in the $m_{1/2}, m_0$ planes for (a) $\tan\beta = 10, \mu < 0$, (b) $\tan\beta = 10, \mu > 0$, (c) $\tan\beta = 35, \mu < 0$, and (d) $\tan\beta = 50, \mu > 0$. The latter are close to the largest values of $\tan\beta$ for which we find generic solutions to the electroweak symmetry-breaking conditions for $\mu < 0$ and > 0, respectively [14]. The double dot-dashed (orange) lines are contours of the spin-independent cross section, and we have indicated the contours $\sigma_{SI} = 10^{-9}$ pb in panels (a, d) and $\sigma_{SI} = 10^{-12}$ pb in panels (b, c). The other bolder contours are for cross sections differing by factors of 10, and the finer contours for cross sections differing by interpolating factors of 3 (in order to ensure clarity, not all of the interpolating contours are displayed).

These cross-section contours are combined in Fig. 1 with other information on the CMSSM parameter space. The lower right-hand corners of the panels are excluded because there the LSP is the lighter $\tilde{\tau}_1$. The light (turquoise) shaded regions are those with $0.1 < \Omega_\chi h^2 < 0.3$ [15]. The 'bulk' regions are clearly visible in panels (a,b) and (d), and coannihilation 'tails' in all panels [14]. For our default choices $A = 0$, $m_t(pole) = 175$ GeV and $m_b(m_b)^{\overline{MS}}_{SM} = 4.25$ GeV, the 'focus-point' regions [22] are at larger values of m_0 than are shown in any of the panels. Rapid-annihilation 'funnels' are visible in panels (c) and (d): that in the former panel bisects the 'bulk' region. The near-vertical dashed (black) lines at small $m_{1/2}$ are the chargino-mass contours $m_{\chi^\pm} = 103.5$ GeV [29], and the near-vertical dotted (red) lines at larger $m_{1/2}$ are the contours $m_h = 114.1$ GeV [9], as calculated using `FeynHiggs` [30]. The large medium (green) shaded regions in panels (a) and (c) are those excluded by $b \to s\gamma$ [18]: smaller excluded regions are also visible in panels (b) and (d) at small $m_{1/2}$. Finally, the sloping shaded (pink) regions in panels (b) and (d) delineate the $\pm 2 - \sigma$ ranges of $g_\mu - 2$ [12], which are absent for the $\mu < 0$ panels (a) and (c).

The LEP lower limits on m_h and $m_{\chi^\pm}$, as well as the experimental measurement of $b \to s\gamma$ for $\mu < 0$, tend to bound the cross sections from above, as we discuss later in more detail. Generally speaking, the spin-independent cross section is relatively large in the 'bulk' region, but falls off in the 'tail' and 'funnel' regions. In the focus-point regions, the spin-independent cross section is relatively independent of m_χ and for $\tan\beta = 10$, takes a value between 10^{-9} and 10^{-8} pb [22, 28]. Also, we note also that there is a strong cancellation in the spin-

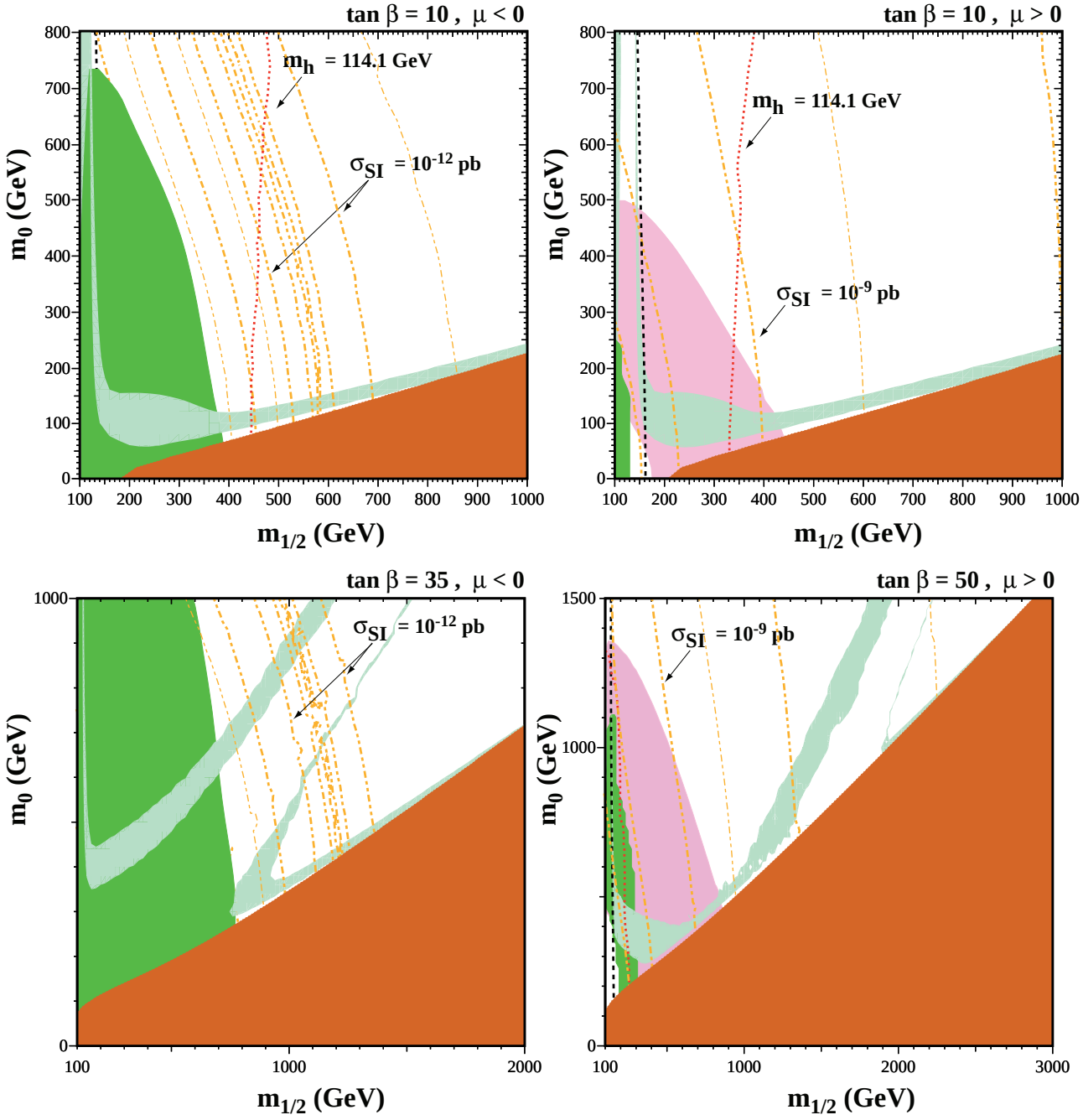

Figure 1: *Spin-independent cross sections in the* $(m_{1/2}, m_0)$ *planes for (a)* $\tan\beta = 10, \mu < 0$, *(b)* $\tan\beta = 10, \mu > 0$, *(c)* $\tan\beta = 35, \mu < 0$ *and (d)* $\tan\beta = 50, \mu > 0$, *assuming* $A_0 = 0, m_t = 175$ *GeV and* $m_b(m_b)^{\overline{MS}}_{SM} = 4.25$ *GeV [14]. The double dot-dashed (orange) curves are contours of the spin-independent cross section, differing by factors of 10 (bolder) and interpolating factors of 3 (finer - when shown). For example, in (b), the curves to the right of the one marked* 10^{-9} *pb correspond to* 3×10^{-10} *pb and* 10^{-10} *pb. The near-vertical lines are the LEP limits* $m_{\chi^\pm} = 103.5$ *GeV (dashed and black) [29],* $m_h = 114.1$ *GeV (dotted and red) [9]. In the dark (brick red) shaded regions, the LSP is the charged* $\tilde{\tau}_1$, *so this region is excluded. The light (turquoise) shaded areas are the cosmologically preferred regions with* $0.1 \leq \Omega_\chi h^2 \leq 0.3$ *[14]. The medium (dark green) shaded regions that are most prominent in panels (a) and (c) are excluded by* $b \to s\gamma$ *[18]. The sloping shaded (pink) regions in panels (b) and (d) delineate the* $\pm 2 - \sigma$ *ranges of* $g_\mu - 2$ *[12].*

independent cross section when $\mu < 0$ [8, 7], as seen along strips in panels (a, c) of Fig. 1 where $m_{1/2} \sim 500, 1100$ GeV, respectively. In the cancellation region, the cross section drops lower than 10^{-14} pb. All these possibilities for suppressed spin-independent cross sections are disfavoured by the data on $g_\mu - 2$ [10, 11, 12], which favour values of $m_{1/2}$ and m_0 that are not very large, as well as $\mu > 0$, as seen in panels (b, d) of Fig. 1. Thus $g_\mu - 2$ tends to provide a lower bound on the spin-independent cross section.

Fig. 2 displays contours of the spin-dependent cross section in the $m_{1/2}, m_0$ planes for (a) $\tan\beta = 10, \mu < 0$, (b) $\tan\beta = 10, \mu > 0$, (c) $\tan\beta = 35, \mu < 0$, and (d) $\tan\beta = 50, \mu > 0$. The dot-dashed (blue) lines are those of the spin-dependent cross section, and the other notation is as in Fig. 1. The bolder lines are contours differing by factors of 10 from the indicated ones, and the finer lines, when shown, differ by interpolating factors of 3. We note again that the cross section is generically larger in the 'bulk' region and smaller in the coannihilation 'tail' and rapid-annihilation 'funnel' regions. In the focus-point regions, the spin-dependent cross-section is also relatively constant and for $\tan\beta = 10$ takes values between 10^{-5} and 10^{-4} pb [22, 28]. Unlike the spin-independent case, there are no cancellations in the spin-dependent cross section.

Fig. 3 illustrates the effect on the cross sections of each of the principal phenomenological constraints, in the particular cases $\tan\beta = 10$ and (a, b) $\mu > 0$, (c, d) $\mu < 0$, (e) $\tan\beta = 35, \mu < 0$ and (f) $\tan\beta = 50, \mu > 0$. The solid (blue) lines mark the bounds on the cross sections allowed by the relic-density constraint $0.1 < \Omega_\chi h^2 < 0.3$ alone [15]. For any given value of $m_{1/2}$, only a restricted range of m_0 is allowed. Therefore, only a limited range of m_0, and hence only a limited range for the cross section, is allowed for any given value of m_χ. The thicknesses of the allowed regions are due in part to the assumed uncertainties in the nuclear inputs. These have been discussed at legnth in [7, 8] and we refer the reader there for details. In the case (e) of $\tan\beta = 35, \mu < 0$ and (f) of $\tan\beta = 50, \mu > 0$, two or three different narrow ranges of m_0 may be allowed for the same value of $m_{1/2}$, but they have quite similar cross sections, as seen already in Figs. 1(c,d) and 2(c,d). On the other hand, a broad range of m_χ is allowed, when one takes into account the coannihilation 'tail' region at each $\tan\beta$ and the rapid-annihilation 'funnel' regions for $\tan\beta = 35, 50$ [14] [3]. The dashed (black) lines in Fig. 3 display the range allowed by the $b \to s\gamma$ constraint [18] alone, which is more important for $\mu < 0$. In this case, a broader range of m_0 and hence the spin-independent cross section is possible for any given value of m_χ. The impact of the constraint due to m_h is shown by the dot-dashed (green) lines in Fig. 3. We implement this constraint by requiring that $m_h > 114.1$ GeV when calculated using the `FeynHiggs` code [30].

[3] We do not show predictions in the 'focus-point' region [22].

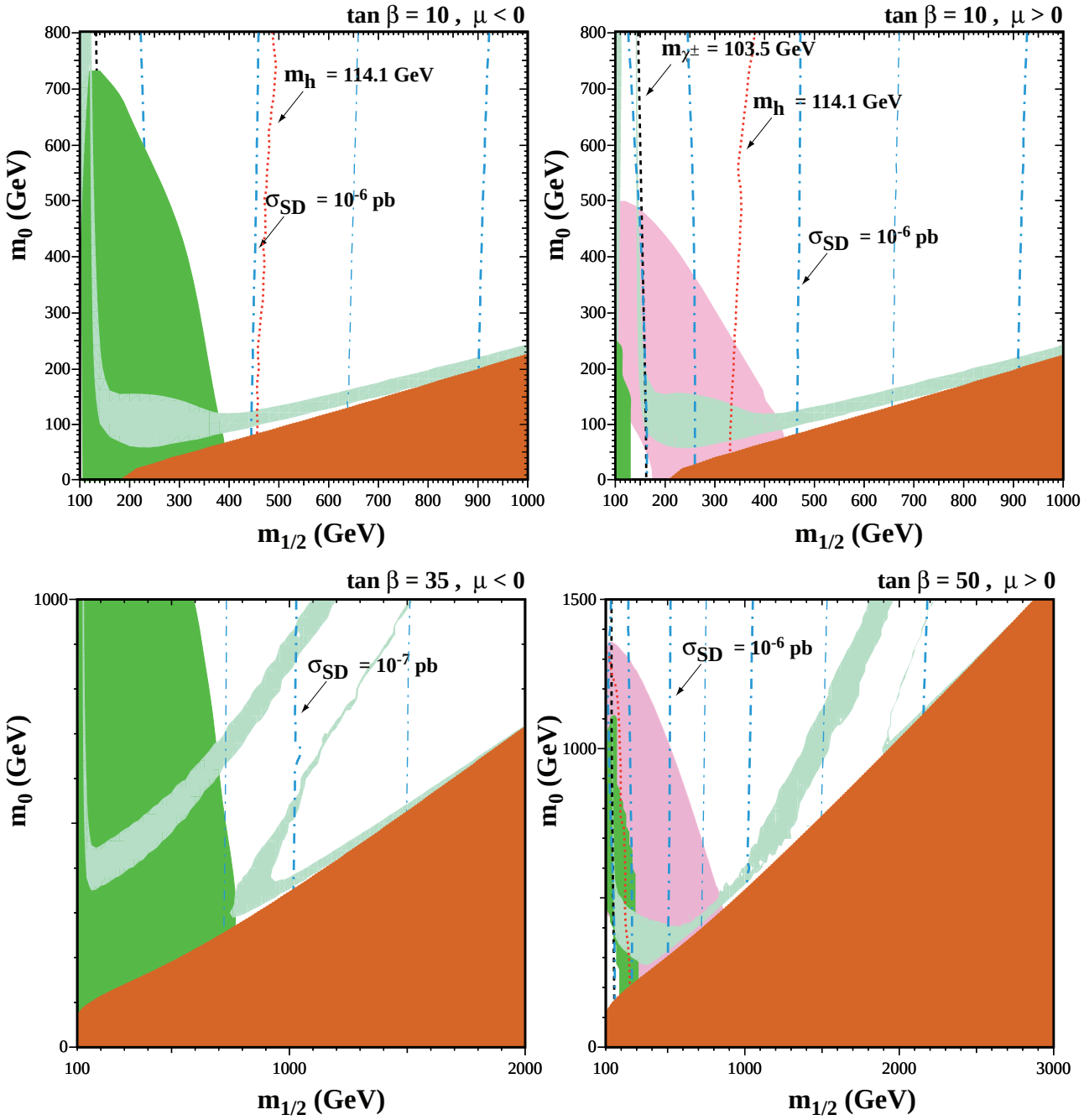

Figure 2: *Spin-dependent cross sections in the* $(m_{1/2}, m_0)$ *planes for (a)* $\tan\beta = 10, \mu < 0$*, (b)* $\tan\beta = 10, \mu > 0$*, (c)* $\tan\beta = 35, \mu < 0$ *and (d)* $\tan\beta = 50, \mu > 0$*, assuming* $A_0 = 0, m_t = 175$ *GeV and* $m_b(m_b)^{\overline{MS}}_{SM} = 4.25$ *GeV [14]. The dot-dashed (blue) lines are contours of the spin-dependent cross section, differing by factors of 10 (bolder) and interpolating factors of 3 (finer - when shown). The near-vertical dashed lines are the LEP limits* $m_{\chi^\pm} = 103.5$ *GeV (black) [29],* $m_h = 114.1$ *GeV (red) [9]. In the dark (brick red) shaded regions, the LSP is the charged* $\tilde{\tau}_1$*, so this region is excluded. The light (turquoise) shaded areas are the cosmologically preferred regions with* $0.1 \leq \Omega_\chi h^2 \leq 0.3$ *[15]. The medium (dark green) shaded regions are excluded by* $b \to s\gamma$ *[18].*

Comparing with the previous constraints, we see that a region at low m_χ is excluded by m_h, strengthening significantly the previous *upper* limit on the spin-independent cross section. Finally, the dotted (red) lines in Fig. 3 show the impact of the $g_\mu - 2$ constraint [12]. This imposes an upper bound on $m_{1/2}$ and hence m_χ, and correspondingly a *lower* limit on the spin-independent cross section.

We emphasize again the important impacts of the updated LEP limits on the chargino and (particularly) Higgs masses. Significantly smaller LSP masses and correspondingly larger cross sections could be found if one used earlier, weaker LEP limits.

The shaded (pale blue) regions in panels (a,b,f) of Fig. 3 show the ranges of m_χ and the cross sections that survive all the phenomenological constraints. We find for $\tan\beta = 10$,

$$135 \text{ GeV} \lesssim m_\chi \lesssim 180 \text{ GeV for } \mu > 0 \tag{1}$$

and the lower limit is $m_\chi \gtrsim 190$ GeV for $\mu < 0$. The upper bound in (1) is due to $g_\mu - 2$, and there is no such upper bound for $\mu < 0$, unless one interprets the LEP 'hint' as a real Higgs signal [9], and imposes $m_h < 117$ GeV, in which case one finds $m_\chi \lesssim 370$ GeV. The ranges of cross sections corresponding to (1) are

$$5 \times 10^{-10} \text{ pb} \lesssim \quad \sigma_{SI} \quad \lesssim 3 \times 10^{-9} \text{ pb}, \tag{2}$$

$$1 \times 10^{-6} \text{ pb} \lesssim \quad \sigma_{SD} \quad \lesssim 4 \times 10^{-6} \text{ pb}, \tag{3}$$

for $\tan\beta = 10$ and $\mu > 0$, and we find

$$\sigma_{SI} \quad \lesssim \quad 2 \times 10^{-11} \text{ pb}, \tag{4}$$

$$\sigma_{SD} \quad \lesssim \quad 1 \times 10^{-6} \text{ pb}, \tag{5}$$

for $\tan\beta = 10$ and $\mu < 0$. No lower limits for the spin-independent cross section are possible with the constraints considered above, both because the $g_\mu - 2$ constraint is inapplicable and must be discarded if this sign of μ is to be considered at all, and also because of the cancellation in σ_{SI} that is visible in panels (a) and (c) of Fig. 1. Even if we take the LEP 'hint' of a signal for a Higgs boson, and impose the upper limit $m_h < 117$ GeV, because the bound on m_χ is past the cancellation region, we find no useful lower bound for $\tan\beta = 10$ and $\mu < 0$. For the spin-dependent cross section, a lower limit due to the relic density is determined by the endpoint of the coannihilation region, namely $\sigma_{SD} \gtrsim 2 \times 10^{-8}$ pb. A Higgs mass bound of 117 GeV in this case would impose $\sigma_{SD} \gtrsim 10^{-7}$ pb.

We see in panel (f) of Fig. 3 that the spin-independent cross section for $\mu > 0$ may be rather larger for $\tan\beta = 50$ than for $\tan\beta = 10$ [16], as shown in panel (a). This analysis is

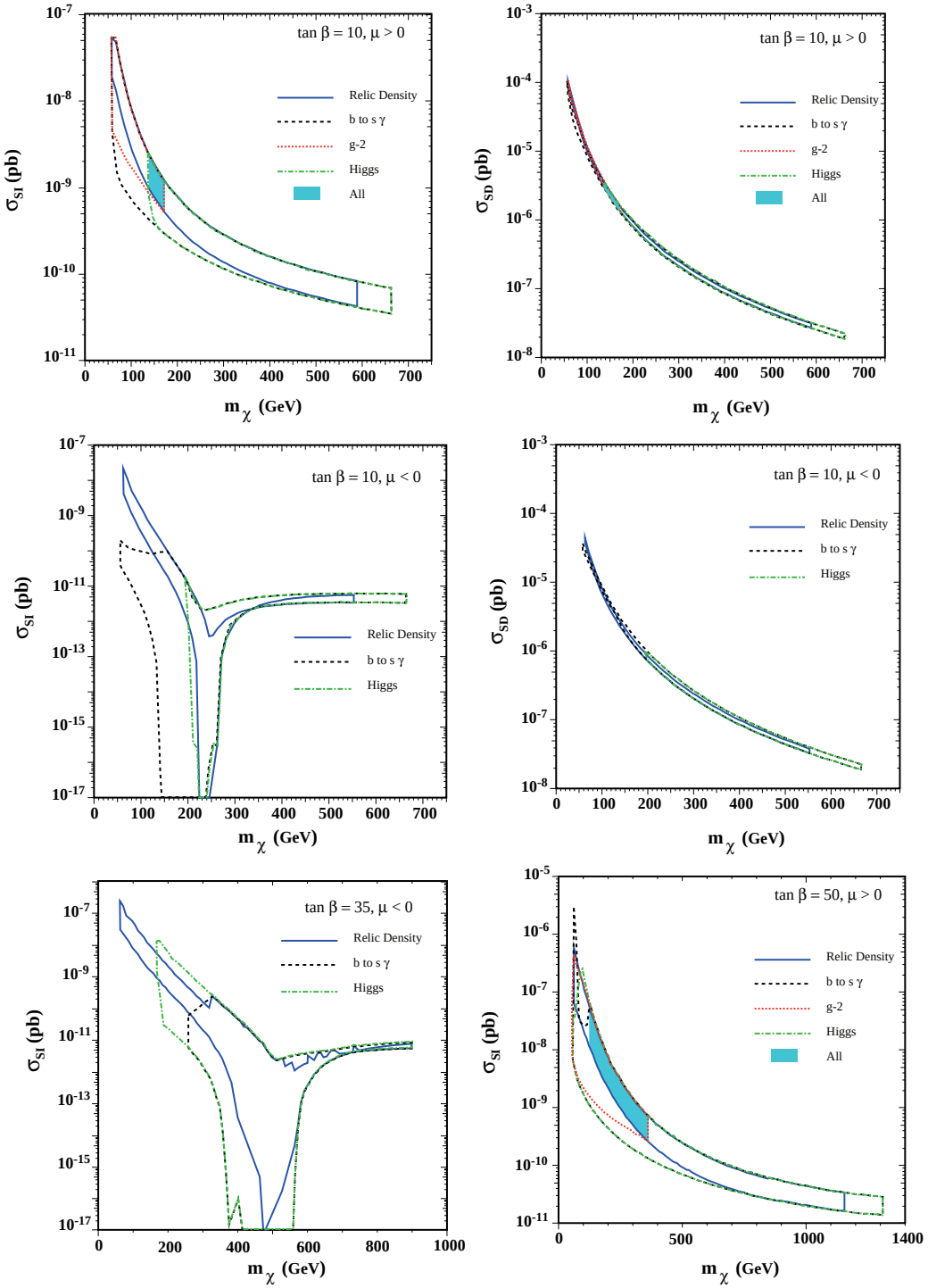

Figure 3: *Allowed ranges of the cross sections for* $\tan\beta = 10$ *and (a, b)* $\mu > 0$*, (c, d)* $\mu < 0$*, for (a, c) spin-independent and (b, d) spin-dependent elastic scattering. Panel (e) shows the spin-independent cross section for* $\tan\beta = 35$ *and* $\mu < 0$*, and panel (f) the spin-independent cross section for* $\tan\beta = 50$ *and* $\mu > 0$*. The solid (blue) lines indicate the relic density constraint [15], the dashed (black) lines the* $b \to s\gamma$ *constraint [18], the dot-dashed (green) lines the* m_h *constraint [9], and the dotted (red) lines the* $g_\mu - 2$ *constraint [12]. The shaded (pale blue) region is allowed by all the constraints.*

extended in panels (a) and (c) of Fig. 4 to all the values $8 < \tan\beta \leq 55$ (below $\tan\beta \simeq 8$ it is not possible to satisfy both the Higgs mass and $g-2$ constraints [11, 12], and above $\tan\beta \simeq 55$ we no longer find consistent CMSSM parameters), and we find overall that

$$2 \times 10^{-10} \text{ pb} \lesssim \quad \sigma_{SI} \quad \lesssim 6 \times 10^{-8} \text{ pb}, \tag{6}$$

$$2 \times 10^{-7} \text{ pb} \lesssim \quad \sigma_{SD} \quad \lesssim 10^{-5} \text{ pb}, \tag{7}$$

for $\tan\beta \leq 55$ and $\mu > 0$. As we see in panels (a) and (c) of Fig. 4, for $\mu > 0$, m_h provides the most important upper limit on the cross sections for $\tan\beta < 23$, and $b \to s\gamma$ for larger $\tan\beta$, with $g_\mu - 2$ always providing a more stringent lower limit than the relic-density constraint. The relic density constraint shown is evaluated at the endpoint of the coannihilation region. At large $\tan\beta$, we have not considered moving far out into the Higgs funnels or the focus-point regions, as their locations are very sensitive to input parameters and calculational details [25]. In the case $\mu < 0$, there is no lower limit on the spin-independent cross section, for the reasons discussed earlier. We find

$$\sigma_{SI} \quad \lesssim 2 \times 10^{-10} \text{ pb}, \tag{8}$$

$$2 \times 10^{-8} \text{ pb} \lesssim \quad \sigma_{SD} \quad \lesssim 2 \times 10^{-6} \text{ pb} \tag{9}$$

for $\mu < 0$ and $5 < \tan\beta \leq 35$ (below $\tan\beta \simeq 5$ it is not possible to satisfy both the Higgs mass and relic density constraints [17], and above $\tan\beta \simeq 35$ we no longer find consistent CMSSM parameters), with the upper limits being imposed by m_h for $\tan\beta < 12$ and by $b \to s\gamma$ for larger $\tan\beta$, as seen in panels (b) and (d) of Fig. 4. The relic-density constraint imposes an interesting lower limit on σ_{SD}, but not on σ_{SI}, as discussed above. Again, requiring $m_h < 117$ GeV would impose a lower limit $\sigma_{SD} \gtrsim 3 \times 10^{-7}$ pb, and since a 117 GeV bound would cut out the cancellation region, we can obtain a lower bound on the spin-independent cross section, $\sigma_{SI} \gtrsim 10^{-11}$ for $\tan\beta = 35$ and $\mu < 0$.

We conclude that the available experimental constraints on CMSSM model parameters greatly restrict the allowed ranges of elastic scattering cross sections for supersymmetric dark matter. Upper limits are imposed on both σ_{SI} and σ_{SD} by both the LEP Higgs constraint and $b \to s\gamma$. If one takes at face value the $g_\mu - 2$ constraint, in addition to requiring $\mu > 0$, it also imposes lower limits on both σ_{SI} and σ_{SD}, providing experiments with a plausible sensitivity to aim for. On the other hand, if one drops the $g_\mu - 2$ constraint and tolerates $\mu < 0$, there is no useful lower limit on σ_{SI}. A lower bound on σ_{SD} is possible if one imposes $m_h < 117$ GeV, motivated by the LEP Higgs 'hint'. The LEP constraints are now stable, but the situation with $g_\mu - 2$ can be expected to clarify soon. If the apparent deviation from

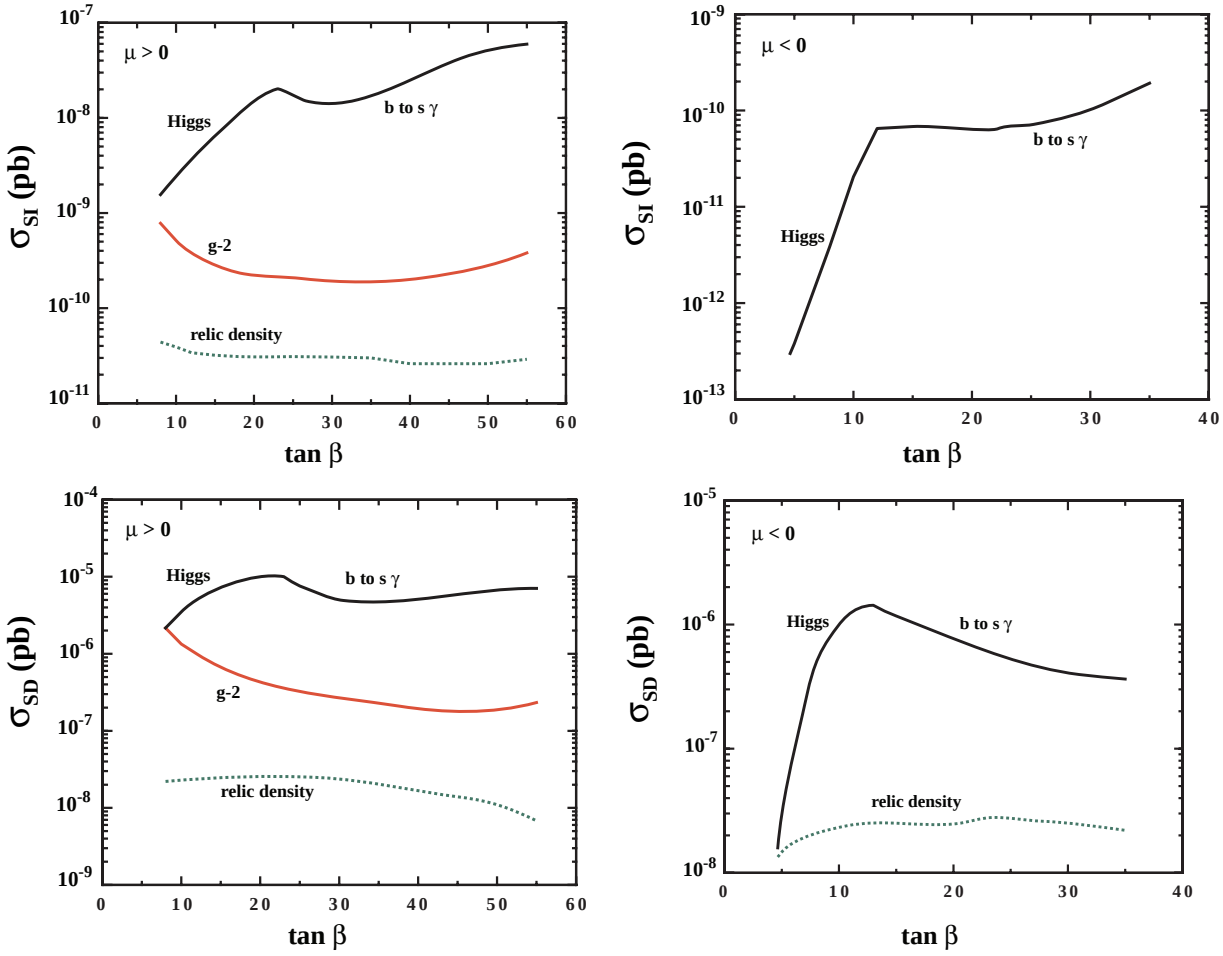

Figure 4: *The allowed ranges of (a, b) the spin-independent cross section and (c, d) the spin-dependent cross section, for (a, c) $\mu > 0$ and (b, d) $\mu < 0$. The darker solid (black) lines show the upper limits on the cross sections obtained from m_h and $b \to s\gamma$, and (where applicable) the lighter solid (red) lines show the lower limits suggested by $g_\mu - 2$ and the dotted (green) lines the lower limits from the relic density.*

the Standard Model [10] is confirmed, direct searches for supersymmetric dark matter may have bright prospects, at least within the CMSSM framework studied here.

Acknowledgments

The work of K.A.O. was supported in part by DOE grant DE–FG02–94ER–40823.

References

[1] J. Ellis, J.S. Hagelin, D.V. Nanopoulos, K.A. Olive and M. Srednicki, Nucl. Phys. B **238**, 453 (1984); see also H. Goldberg, Phys. Rev. Lett. **50**, 1419 (1983).

[2] M.W. Goodman and E. Witten, Phys. Rev. D **31**, 3059 (1986).

[3] For a review, see, e.g., G. Jungman, M. Kamionkowski and K. Griest, Phys. Rep. **267**, 195 (1996).

[4] R. Bernabei *et al.*, DAMA Collaboration, Phys. Lett. B **480**, 23 (2000).

[5] H. V. Klapdor-Kleingrothaus, arXiv:hep-ph/0104028.

[6] K. Griest, Phys. Rev. D **38**, 2357 (1988); J. Ellis and R. Flores, Nucl. Phys. B **307**, 883 (1988); R. Barbieri, M. Frigeni and G. Giudice, Nucl. Phys. B **313**, 725 (1989); R. Flores, K.A. Olive and M. Srednicki, Phys. Lett. B **237**, 72 (1990); J. Ellis and R. Flores, Phys. Lett. B **263**, 259 (1991); J. Ellis and R. Flores, Phys. Lett. B **300**, 175 (1993); M. Drees and M. M. Nojiri, Phys. Rev. D **48**, 3483 (1993); V. Bednyakov, H.V. Klapdor-Kleingrothaus and S. Kovalenko, Phys. Rev. D **50**, 7128 (1994); R. Arnowitt and P. Nath, Phys. Rev. D **54**, 2374 (1996) [arXiv:hep-ph/9509260]; H. Baer and M. Brhlik, Phys. Rev. D **57**, 567 (1998) [arXiv:hep-ph/9706509]; E. Accomando, R. Arnowitt, B. Dutta and Y. Santoso, Nucl. Phys. B **585**, 124 (2000) [arXiv:hep-ph/0001019]; A. Corsetti and P. Nath, hep-ph/0003186.

[7] J. Ellis, A. Ferstl and K. A. Olive, Phys. Rev. D **63**, 065016 (2001) [arXiv:hep-ph/0007113].

[8] J. Ellis, A. Ferstl and K. A. Olive, Phys. Lett. B **481**, 304 (2000) [arXiv:hep-ph/0001005].

[9] LEP Higgs Working Group for Higgs boson searches, OPAL Collaboration, ALEPH Collaboration, DELPHI Collaboration and L3 Collaboration, *Search for the Standard Model Higgs Boson at LEP*, ALEPH-2001-066, DELPHI-2001-113, CERN-L3-NOTE-2699, OPAL-PN-479, LHWG-NOTE-2001-03, CERN-EP/2001-055, arXiv:hep-ex/0107029; *Searches for the neutral Higgs bosons of the MSSM: Preliminary combined results using LEP data collected at energies up to 209 GeV*, LHWG-NOTE-2001-04, ALEPH-2001-057, DELPHI-2001-114, L3-NOTE-2700, OPAL-TN-699, arXiv:hep-ex/0107030.

[10] H. N. Brown *et al.* [Muon g-2 Collaboration], Phys. Rev. Lett. **86**, 2227 (2001) [hep-ex/0102017].

[11] L. L. Everett, G. L. Kane, S. Rigolin and L. Wang, Phys. Rev. Lett. **86**, 3484 (2001) [arXiv:hep-ph/0102145]; J. L. Feng and K. T. Matchev, Phys. Rev. Lett. **86**, 3480 (2001) [arXiv:hep-ph/0102146]; E. A. Baltz and P. Gondolo, Phys. Rev. Lett. **86**, 5004 (2001) [arXiv:hep-ph/0102147]; U. Chattopadhyay and P. Nath, Phys. Rev. Lett. **86**, 5854 (2001) [arXiv:hep-ph/0102157]; S. Komine, T. Moroi and M. Yamaguchi, Phys. Lett. B **506**, 93 (2001) [arXiv:hep-ph/0102204]; S. P. Martin and J. D. Wells, Phys. Rev. D **64**, 035003 (2001) [arXiv:hep-ph/0103067]; H. Baer, C. Balazs, J. Ferrandis and X. Tata, Phys. Rev. D **64**, 035004 (2001) [arXiv:hep-ph/0103280]; W. de Boer, M. Huber, C. Sander and D. I. Kazakov, Phys. Lett. B **515**, 283 (2001); R. Arnowitt, B. Dutta, B. Hu and Y. Santoso, Phys. Lett. B **505**, 177 (2001) [arXiv:hep-ph/0102344].

[12] J. Ellis, D. V. Nanopoulos and K. A. Olive, Phys. Lett. B **508**, 65 (2001) [arXiv:hep-ph/0102331].

[13] For other scattering calculations, see, for example: A. Bottino, F. Donato, N. Fornengo and S. Scopel, Phys. Rev. D **63**, 125003 (2001) [arXiv:hep-ph/0010203]; M. Drees, Y. G. Kim, T. Kobayashi and M. M. Nojiri, Phys. Rev. D **63**, 115009 (2001) [arXiv:hep-ph/0011359]; Y. G. Kim and M. M. Nojiri, arXiv:hep-ph/0104258; A. B. Lahanas, D. V. Nanopoulos and V. C. Spanos, Mod. Phys. Lett. A **16**, 1229 (2001) [arXiv:hep-ph/0009065]; A. B. Lahanas, D. V. Nanopoulos and V. C. Spanos, Phys. Lett. B **518**, 94 (2001) [arXiv:hep-ph/0107151]. M. E. Gomez and J. D. Vergados, Phys. Lett. B **512**, 252 (2001) [arXiv:hep-ph/0012020].

[14] J. R. Ellis, T. Falk, G. Ganis, K. A. Olive and M. Srednicki, Phys. Lett. B **510**, 236 (2001) [arXiv:hep-ph/0102098].

[15] N. Bahcall, J. P. Ostriker, S. Perlmutter and P. J. Steinhardt, Science **284**, 1481 (1999).

[16] R. Arnowitt, B. Dutta and Y. Santoso, arXiv:hep-ph/0008336.

[17] J. R. Ellis, G. Ganis, D. V. Nanopoulos and K. A. Olive, Phys. Lett. B **502**, 171 (2001) [arXiv:hep-ph/0009355]. A. Bottino, N. Fornengo and S. Scopel, Nucl. Phys. B **608**, 461 (2001) [arXiv:hep-ph/0012377].

[18] CLEO Collaboration, S. Chen *et al.*, CLEO CONF 01-16, submitted to Phys. Rev. D; BELLE Collaboration, BELLE-CONF-0003, contribution to the 30th International conference on High-Energy Physics, Osaka, 2000. See also K. Abe *et al.*, [Belle Collaboration], arXiv:hep-ex/0107065; L. Lista [BaBar Collaboration], arXiv:hep-ex/0110010; G. Degrassi, P. Gambino and G. F. Giudice, JHEP **0012**, 009 (2000) [arXiv:hep-ph/0009337]; see also M. Carena, D. Garcia, U. Nierste and C. E. Wagner, Phys. Lett. B **499**, 141 (2001) [arXiv:hep-ph/0010003].

[19] P. Nath and R. Arnowitt, Phys. Rev. Lett. **74**, 4592 (1995); F. M. Borzumati, M. Drees and M. M. Nojiri, Phys. Rev. D **51**, 341 (1995) [arXiv:hep-ph/9406390]; L. Bergstrom and P. Gondolo, Astropart. Phys. **5**, 263 (1996) [arXiv:hep-ph/9510252]; H. Baer and M. Brhlik, Phys. Rev. D **55**, 3201 (1997) [arXiv:hep-ph/9610224]; H. Baer, M. Brhlik, D. Castano and X. Tata, Phys. Rev. D **58**, 015007 (1998) [arXiv:hep-ph/9712305]; W. de Boer, H. J. Grimm, A. V. Gladyshev and D. I. Kazakov, Phys. Lett. B **438**, 281 (1998) [arXiv:hep-ph/9805378]; W. de Boer, M. Huber, A. V. Gladyshev and D. I. Kazakov, Eur. Phys. J. C **20**, 689 (2001) [arXiv:hep-ph/0102163].

[20] K. Griest and D. Seckel, Phys. Rev. D **43**, 3191 (1991); S. Mizuta and M. Yamaguchi, Phys. Lett. B **298**, 120 (1993) [arXiv:hep-ph/9208251]; J. Edsjo and P. Gondolo, Phys. Rev. D **56**, 1879 (1997) [arXiv:hep-ph/9704361]. C. Boehm, A. Djouadi and M. Drees, Phys. Rev. D **62**, 035012 (2000) [arXiv:hep-ph/9911496].

[21] J. Ellis, T. Falk and K.A. Olive, Phys. Lett. B **444**, 367 (1998); J. Ellis, T. Falk, K.A. Olive and M. Srednicki, Astropart. Phys. **13**, 181 (2000); M. E. Gómez, G. Lazarides and C. Pallis, Phys. Rev. D **61**, 123512 (2000) [arXiv:hep-ph/9907261] and Phys. Lett. B **487**, 313 (2000) [arXiv:hep-ph/0004028]; R. Arnowitt, B. Dutta and Y. Santoso, Nucl. Phys. B **606**, 59 (2001) [arXiv:hep-ph/0102181].

[22] J. L. Feng, K. T. Matchev and T. Moroi, Phys. Rev. Lett. **84**, 2322 (2000) [arXiv:hep-ph/9908309]; J. L. Feng, K. T. Matchev and T. Moroi, Phys. Rev. D **61**, 075005 (2000) [arXiv:hep-ph/9909334]; J. L. Feng, K. T. Matchev and F. Wilczek, Phys. Lett. B **482**, 388 (2000) [arXiv:hep-ph/0004043].

[23] M. Drees and M. M. Nojiri, Phys. Rev. D **47**, 376 (1993); H. Baer and M. Brhlik, Phys. Rev. D **53**, 597 (1996) and Phys. Rev. D **57**, 567 (1998); H. Baer, M. Brhlik, M. A. Diaz, J. Ferrandis, P. Mercadante, P. Quintana and X. Tata, Phys. Rev. D **63**, 015007 (2001). A. B. Lahanas and V. C. Spanos, arXiv:hep-ph/0106345.

[24] Information about this code is available from K. A. Olive: it contains important contributions from T. Falk, G. Ganis, J. McDonald, K. A. Olive and M. Srednicki.

[25] J. R. Ellis and K. A. Olive, Phys. Lett. B **514**, 114 (2001) [arXiv:hep-ph/0105004].

[26] A. B. Lahanas, D. V. Nanopoulos and V. C. Spanos, Phys. Rev. D **62**, 023515 (2000) [arXiv:hep-ph/9909497]; V. Barger and C. Kao, Phys. Lett. B **518**, 117 (2001) [arXiv:hep-ph/0106189]; L. Roszkowski, R. Ruiz de Austri and T. Nihei, JHEP **0108**, 024 (2001) [arXiv:hep-ph/0106334]; A. Djouadi, M. Drees and J. L. Kneur, JHEP **0108**, 055 (2001) [arXiv:hep-ph/0107316].

[27] G. Jungman, M. Kamionkowski and K. Griest, `http://t8web.lanl.gov/people/jungman/neut-package.html`.

[28] J. Ellis, J. L. Feng, A. Ferstl, K. T. Matchev and K. A. Olive, arXiv:astro-ph/0110225.

[29] Joint LEP 2 Supersymmetry Working Group, *Combined LEP Chargino Results, up to 208 GeV*, `http://lepsusy.web.cern.ch/lepsusy/www/inos_moriond01/charginos_pub.html`.

[30] S. Heinemeyer, W. Hollik and G. Weiglein, Comput. Phys. Commun. **124**, 76 (2000) [arXiv:hep-ph/9812320]; S. Heinemeyer, W. Hollik and G. Weiglein, Eur. Phys. J. C **9**, 343 (1999) [arXiv:hep-ph/9812472].